

PROF. WEIXING SHAN (Orcid ID : 0000-0001-7286-4041)

Article type : Regular Manuscript

***Phytophthora infestans* RXLR effector PITG20303 targets a potato MKK1 protein to suppress plant immunity**

Yu Du^{1,*}, Xiaokang Chen^{1,*}, Yalu Guo^{1,*}, Xiaojiang Zhang¹, Houxiao Zhang¹, Fangfang Li¹, Guiyan Huang^{3,4}, Yuling Meng² & Weixing Shan^{2,#}

¹State Key Laboratory of Crop Stress Biology for Arid Areas and College of Horticulture, Northwest A&F University, Yangling, Shaanxi 712100, China.

²State Key Laboratory of Crop Stress Biology for Arid Areas and College of Agronomy, Northwest A&F University, Yangling, Shaanxi 712100, China.

³College of Life Sciences, Northwest A&F University, Yangling, Shaanxi 712100, China.

⁴China-USA Citrus Huanglongbing Joint Laboratory, National Navel Orange Engineering Research Center, College of Life Sciences, Gannan Normal University, Ganzhou 341000, China.

ORCID IDs: 0000-0002-3512-0200 (Y.D.); 0000-0001-7286-4041 (W.S.).

* These authors contributed equally to this work.

Corresponding author: Weixing Shan (E-mail: wxshan@nwfau.edu.cn; Tel: (0086) 029-87082990)

Received: 17 January 2020

Accepted: 27 July 2020

This article has been accepted for publication and undergone full peer review but has not been through the copyediting, typesetting, pagination and proofreading process, which may lead to differences between this version and the [Version of Record](#). Please cite this article as [doi: 10.1111/NPH.16861](https://doi.org/10.1111/NPH.16861)

This article is protected by copyright. All rights reserved

Summary

·Pathogens secrete a plethora of effectors into the host cell to modulate plant immunity. Analysing the role of effectors in altering the function of their host target proteins will reveal critical components of the plant immune system.

·Here we show that *Phytophthora infestans* RXLR effector PITG20303, a virulent variant of AVRblb2 (PITG20300) that escapes the recognition by the resistance protein Rpi-blb2, suppresses PAMP-triggered immunity (PTI) and promotes pathogen colonization by targeting and stabilizing a potato MAPK cascade protein, StMKK1. Both PITG20300 and PITG20303 target StMKK1, as confirmed by multiple *in vivo* and *in vitro* assays, and *StMKK1* was shown as a negative regulator of plant immunity as determined by overexpression and gene silencing.

·*StMKK1* is a negative regulator of plant PTI, and the kinase activities of StMKK1 is required for its suppression of PTI and effector interaction. PITG20303 partially depends on MKK1, PITG20300 does not depend on MKK1 for suppression of PTI-induced ROS burst, while the full virulence activities of nuclear targeted PITG20303 and PITG20300 are dependent on MKK1.

·Our results show that PITG20303 and PITG20300 target and stabilize the plant MAPK cascade signalling protein StMKK1 to negatively regulate plant PTI response.

Key words:

Effector targets, MAPK cascade, Oomycete, *Phytophthora infestans*, Pathogenicity, Susceptibility

Introduction

Phytophthora infestans is a notorious oomycete plant pathogen, which causes late blight on potato and tomato and is a serious threat to food security. To enable infection it secretes a plethora of effectors into host cells to modulate host immune response and facilitate infection (Haas et al., 2009). RXLR effectors belong to the largest group of effectors, are only found in oomycete pathogens and are defined by a conserved Arg-X-Leu-Arg (RXLR) motif at their N-terminus. The RXLR motif is required for effector host translocation (Kale et al., 2010). RXLR effectors exploit diverse machineries to manipulate plant cellular processes, e.g. inhibit plant ER-stress mediated immunity (Fan et al., 2018), disturb plant PTI (PAMP triggered immunity) responses (Zheng et al., 2018; Bouwmeester et al., 2011), target plant defence negative regulators (Boevink et al., 2016; Wang et al., 2015; Yang et al., 2016; He et al., 2018), suppress host cell death (Jing et al., 2016), interfere with protein secretion (Bozkurt et al., 2011; Du et al., 2015a; Tomczynska et al., 2018), interfere with plant RNA silencing process (Qiao et al., 2015; Vetukuri et al., 2017), and regulate plant transcription (McClellan et al., 2013; Kong et al., 2017; Turnbull et al., 2017).

Plants have evolved multi-layered immune systems to recognize and combat pathogens. The first layer of plant defense are the plasma membrane localized pattern recognition receptors (PRRs), which detect the conserved molecules of microbes known as pathogen/microbe-associated molecular patterns (PAMPs/MAMPs) (Jones and Dangl, 2006; Zipfel, 2008), and thus activate PAMP-triggered immunity (PTI). As a consequence, pathogens have evolved a plethora of small-secreted effectors to interfere with plant PTI responses, leading to effector-triggered susceptibility. To combat the role of the effectors a second layer of plant defense is conferred by intercellular nucleotide-binding leucine-rich repeat receptors (NLR) known as resistance proteins, which recognize the presence of specific pathogen effectors and activate effector-triggered immunity (ETI) (Hardham and Cahill, 2010; Du et al., 2015b).

Upon PTI activation, plasma membranes localized PRRs sense the pathogen PAMPs or MAMPs and activate MAPK (Mitogen Activated Protein Kinase) cascades to signal to the nucleus to activate an immune response (Ingle et al., 2006). MAPK cascades contain a MAPK kinase kinase (MAPKKK, MEKK or MAP3K), a MAPK kinase (MAPKK, MEK or MAP2K) and a MAPK. Upon PTI response, the MAPKKKs are activated and phosphorylated MKKs that then phosphorylate MAPKs. At least two MAPK cascades that consist of MEKK1-MKK4/5-MPK3/6 and MEKK1-MKK1/2-MPK4 were activated during flg22-triggered PTI response (Zhang et al., 2017). The role of MPK cascade proteins in plant immunity is subtle with different experimental approaches suggesting differing outcomes. For example, MPK4 was previously shown to

positively regulate plant immunity and was phosphorylated by MKK1/2 (Zhang et al., 2012; Zhang et al., 2017). However, the constitutively active MPK4 was shown to negatively regulate plant immunity (Berriri et al., 2012), and MPK4 was also shown to phosphorylate ASR3 to repress flg22-induced gene expression (Li et al., 2015).

MAP kinase signalling components have been shown common effector targets (Bi and Zhou, 2017). Many bacterial effectors are reported to target the flg22 activated MAPK cascade proteins to inhibit plant PTI response (Ling et al., 2017; Zhang et al., 2007, 2012). They either manipulate MAPKKs or proteins upstream of MAPKKs to disturb PRR-mediated resistance (Li et al., 2016; Feng et al., 2012; Zhang et al., 2010; He et al., 2006), or directly target and suppress the activity of MAPKKs downstream signalling components MAPKK or MAPK (Teper et al., 2018; Eschen-Lippold et al., 2016; Wang et al., 2010; Cui et al., 2010). For instance, *Pseudomonas syringae* type III effector HopB1 and HopF2 perturb plant PTI upstream of MAPKKK by targeting BAK1 (Li et al., 2016; Zhou et al., 2014), AvrPphB inhibits PTI via cleaving PBL kinases (Zhang et al., 2010), and the *Xanthomonas campestris* type III effector AvrAC enhances pathogen virulence by targeting and inhibiting the activities of BIK1 and RIPK (Feng et al., 2012). The *Xanthomonas euvesicatoria* type III effector XopAU targets and activates MKK2 to promote pathogen disease (Teper et al., 2018) and in *P. syringae* effector AvrRpt2 represses MPK4/MPK11 activation (Eschen-Lippold et al., 2016), while effectors HopF2 and HopAI1 target and inhibit the kinase activity of AtMKK5 and MPK3/MPK6/MPK4 respectively to inhibit PTI (Wang et al., 2010; Zhang et al., 2007; Zhang et al., 2012). Recently, it has been shown that tomato yellow leaf curl China virus betasatellite protein β C1 targets and inhibits the kinase activities of MKK2 and MPK4 to counter host defense (Hu et al., 2019).

Several oomycete RXLR effectors have been reported to suppress plant PTI responses (Bos et al., 2010; Saunders et al., 2012; Dagdas et al., 2016; Zheng et al., 2018). However, few of them are known to target MAPKKs and interfere with MAP kinase signalling, e.g. *P. infestans* RXLR effector Pi22926, PexRD2 and Pi17316 were found to target host StMAP3K β 2, MAPKK ϵ and MAP3K StVIK, respectively (Ren et al., 2019; King et al., 2014; Murphy et al., 2018). *P. sojae* Avh331 was shown to inhibit the MAPK signalling pathway, however, no physical association of Avh331 and MAPK signalling proteins was demonstrated (Cheng et al., 2012).

The *P. infestans* RXLR effector PITG20303, is a virulent variant of AVRblb2 (PITG20300), harbouring an amino acid alteration from Ala/Ile/Val to Phe at position 69 enabling it to escape the recognition by the broad spectrum resistance protein Rpi-blb2 (Oliva et al., 2015; Vleeshouwers et al., 2011; Haverkort et al., 2016). The AVRblb2 effector family contains four potential variants and different numbers are present in different *P. infestans* isolates, which implies an important role in pathogenicity and that variants may evade recognition by RPI-blb2 or

manipulate different host targets. PITG20303 was found to localize in the host nucleus and more weakly to the plasma membrane to interfere with plant PTI response and promote *P. infestans* colonization (Zheng et al., 2014) which is in contrast to PITG20300 (AVRblb2), which localizes to the host plasma membrane and prevents the secretion of a cysteine proteinase C14 to the apoplast (Bozkurt et al., 2011). Thus, we hypothesize that PITG20303 utilizes a different virulence mechanism from that reported for PITG20300. Here we show that both PITG20303 and PITG20300 suppress plant PTI response and target a potato StMKK1 protein. Silencing and overexpression experiments show that *StMKK1* negatively regulates plant PTI. The kinase activity of StMKK1 is required for its negative regulation of plant defence and effector interaction. StMKK1 is largely dependent by PITG20303 for its virulence activity, and it is fully required for the virulence activity of the nuclear targeted PITG20303NLS and PITG20300NLS. Thus we propose *P. infestans* RXLR effector PITG20303 and PITG20300 target and stabilize a plant resistance negative regulator StMKK1 to suppress plant immunity.

Material and methods

Plasmid Construction

For Y2H assays *PITG20303* was cloned into the pGBKT7 vector using *EcoRI* and *BamHI* sites to form the bait plasmid BD-20303. StMKK1 (Sotub12g010200) was amplified from cDNA generated from potato cultivar Qingshu9, and cloned into the pGADT7 vector using *EcoRI* and *BamHI* sites to form the AD-StMKK1 plasmid. The plasmids used for co-immunoprecipitation (Co-IP) assays were generated by cloning of *PITG20303* or *PITG04097* genes under the control of the 35S promoter in the pART27-N7myc vector (Fan et al., 2018) using *EcoRI* and *XbaI* sites to form myc-20303 and myc-04097 plasmids. StMKK1 was fused to GFP by cloning into the pART27-NGFP vector (Fan et al., 2018) using *EcoRI* and *XbaI* sites to form the GFP-StMKK1 plasmids. For firefly luciferase complementation imaging (LCI) assays, *StMKK1* and *PITG20303* were cloned into pCAMBIA-NLuc and pCAMBIA-CLuc (Chen et al., 2007) using *KpnI* and *SalI* sites to form the StMKK1-nluc and cluc-20303 plasmids, respectively. For bimolecular fluorescence complementation (BiFC) assays *StMKK1* was cloned into pDEST-VYCE(R)^{GW} vector using *StuI* and *KpnI* sites to form the YC-StMKK1 plasmid. *PITG20303*, *PITG04097*, *PITG20300* were cloned into pDEST-VYNE(R)^{GW} vector using *SpeI* and *XhoI* sites to form the YN-20303, YN-04097 and YN-20300 plasmids, respectively. To generate the YN-AVR3a plasmid, *PiAVR3a* was cloned into pDEST-VYNE(R)^{GW} vector using *StuI* and *KpnI* sites. To generate the cluc-20303 and StMKK1-nluc plasmids, *PITG20303* and *StMKK1* were cloned into pCAMBIA1300 vector using *KpnI* and *SalI* sites. For co-localization assays, GFP-20303, GFP-20300, mCherry-

20303, mCherry-20300 and mCherry plasmids were generated in a similar way using *EcoR*I and *Xba*I sites into pART27-NGFP, pART27-NmCherry vectors (Fan et al., 2018), respectively. For *in vitro* kinase activity assays, GFP, StMKK1 or StMKK1^{K99M} were cloned into pET32a vector using *Nco*I and *Xho*I sites to make His-GFP, His-StMKK1 and His-StMKK1^{K99M} plasmids. StMPK4 (Sotub08g028940.1.1) was amplified from cDNA generated from potato cultivar Tianshu11, and cloned into pGEX-6P-1 vector using *Bam*HI and *Sal*I sites to form the GST-StMPK4 plasmid. All the fragments for cloning and all the point mutations were PCR generated and the relevant primers are listed in the Supplemental Table 1.

Plant Growth Condition and Pathogen Infection Assays

Nicotiana benthamiana plants were grown under standard glasshouse conditions. Five weeks old plants were used for infection assays. *P. infestans* isolate 14-3-GFP was grown on rye Suc agar plates at 16-18°C for 9-12 days before zoospores were harvested and used for infection. *Phytophthora parasitica* were cultured as described by Fan et al. (2018). Infection assays were performed according to method described by Champouret et al. (2009). Pathogen inoculated leaves were kept in moisture at 18 °C for 5 or 6 days for *P. infestans* and at 23 °C for 2 or 3 days for *P. parasitica* before lesion diameters were measured.

Agroinfiltration and VIGS

Agrobacterium tumefaciens strain C58C1 carrying binary transformation vectors was grown in liquid LB medium with appropriate antibiotics at 28 °C for two days before centrifugation and resuspension in infiltration medium as described (Champouret et al., 2009). The *Agrobacterium* suspensions were adjusted to OD₆₀₀ of 0.1 for confocal microscope and BiFC assays and 0.3 for Co-IP and infection assays. For co-expression assays *Agrobacterium* cultures carrying different vectors were mixed in a 1:1 ratio before infiltration.

For selection of target sequence for VIGS, we mined the MKK1/2 protein sequences in Sol genomics network database (<https://solgenomics.net/>), and identified four genes encoding *MKK1* in *N. benthamiana*. We selected two cDNA fragments, *MKKseq1* targets two highly conserved genes *Niben101Scf10103g03014* and *Niben101Scf00611G07010* and *MKKseq2* targets *Niben101Scf02790g03012* and *Niben101Scf13387g00027*. We fused these fragments to form the TRV-*NbMKK1* construct. Sequence alignment is shown in Supplemental Figure 6 (see later). TRV-*GUS* was used as control (Tameling and Baulcombe, 2007). Primers used in this assay were shown in Supplemental Table 1. *Agrobacterium* cultures containing TRV2 and TRV1 mixed in a 1:1 ratio with OD₆₀₀ of 1 were infiltrated into the first two leaves of two-week-old *N.*

benthamiana. The fifth and sixth leaves from the bottom were used for infection assays at three weeks after VIGS inoculation.

Flg22 Treatments and ROS production

Leaves from 4-week-old *N. benthamiana* plants were infiltrated with 10 μ M flg22 solution. Samples for qRT-PCR were collected at 3 hours after flg22 treatment. ROS production analysis was performed according to the method Li et al. (2016).

Gene Expression Assay

Total RNA was extracted using TRIzol reagent (Invitrogen). First strand cDNA was synthesized using 1 μ g of RNA by PrimeScript™ RT reagent Kit (TaKaRa) according to the manufacturer's instructions. The cDNA was diluted 20 times and 5 μ l of the diluted cDNA was used as template per PCR with SYBR Green master mix (Roche). qRT-PCR was run on a iQ7 Real-Time Cycler (Life technologies). Gene expression was quantified using the Delta Delta Ct method and normalized to a housekeeping gene actin for *N. benthamiana*. To assess gene silencing efficiency, primer pairs were designed beyond the VIGS targeted sequence (Supplemental Table 1).

Co-immunoprecipitation and Western Blot Analysis

Agroinfiltrated *N. benthamiana* leaves were harvested at two dpi and used for total protein extraction. GTEN buffer (10% glycerol, 25 mM Tris pH 7.5, 150 mM NaCl, 1 mM EDTA) with 1 \times protease inhibitor cocktail (Sigma) and 1% Nonidet P-40 (IGEPAL CA-630) were used for protein extraction. For Co-IP assays, 15 μ l of GFP-trap_A beads (Chromotek) was added to a 1.6 ml of total protein extract, and the mixtures were incubated at 4°C for two hours. Subsequently, the mixtures were spun down at 4°C and the proteins attached to the beads were collected and washed several times. Finally, 100 μ l of protein complex solutions were boiled with loading buffer (300 mM Tris-HCl, pH 6.8, 8.7% SDS, 5% β -mercaptoethanol, 30% glycerol, and 0.12 mg per mL bromophenol blue) for 5-10 min.

For protein stability assays, 1 mg MG132 was dissolved in 0.1 mL DMSO, and then use dH₂O to bring the volume to 21 mL to obtain the concentration of 100 μ M. For control treatments, 0.1 mL DMSO was diluted to the volume of 21 mL using dH₂O. *Myc-StMKK1* was co-agroinfiltrated with *GFP-20303*, *GFP-20300* or *GFP* into *N. benthamiana* leaves and 36 hours after agroinfiltration, the MG132 or its solvent DMSO solutions were infiltrated to the leaves and at 48 hours after agroinfiltration, leaves were harvested and used for protein isolation and western blot analysis. For western blot analysis, proteins were separated on SDS-PAGE gel and

then transferred to an Immune-Blot PVDF membrane (Roche). The membranes were then blocked in blocking buffer TBST (pH 7.2, TBS, 0.05% Tween 20 (Sigma)) with 5% non-fat dry milk with gentle shaking at room temperature for 1.5 hours. Specific antibodies anti-GFP (#AE012, ABclonal), anti-myc (#AE010, ABclonal), anti-mCherry monoclonal antibody (Abbkine) were added into blocking buffer at 1:2000 dilution. Membranes were incubated with antibodies for 1.5 hours at room temperature with gentle shaking. Subsequently the membranes were washed 5 times and then incubated with appropriate secondary antibodies with the same dilution. The secondary antibodies used were HRP Goat anti-Mouse IgG (H+L) antibody (#AS013, ABclonal) and HRP goat anti-rabbit IgG (H+L) antibody (#AS014, ABclonal). Protein bands were detected using eECL western blot kit (CWBio, Beijing, China).

The plasma membrane and nuclear proteins were isolated using the plant plasma membrane isolation kit (BB-3152-1, BestBio, Shanghai, China) and plant nuclear protein isolation kit (BB-3154-1, BestBio, Shanghai, China).

Recombinant Protein Purification and In Vitro Phosphorylation Assays

The constructs of *His-StMKK1*, *His-StMKK1^{K99M}*, *His-GFP* and *GST-StMPK4* were transformed into *Escherichia coli* strain BL21. Proteins were expressed and purified as described (Fan et al., 2018). For *in vitro* phosphorylation assay, 2 µg each of His-StMKK1, His-StMKK1^{K99M}, His-GFP were incubated with 2 µg GST-StMPK4, respectively, with 80 µl reaction buffer, according to the method described by Li et al. (2014b). The phosphorylation of StMPK4 was detected using anti-pERK antibodies (#4370, Cell Signaling).

Y2H Assays

The AD library plasmids were transformed into *Saccharomyces cerevisiae* strain AH109. The bait plasmid pGBKT7-20303 were transformed into *S. cerevisiae* strain Y187. Yeast mating and Y2H screening were performed according to the Matchmaker™ GAL4 Two-Hybrid System 3 & Libraries User Manual (Clontech). For the Y2H assay, pGBKT7 and pGADT7 vectors were co-transformed into the yeast strain AH109. Transformations were checked on SD/-Trp-Leu medium and interactions were confirmed by the gain of α-galactosidase activity (α-gal). Yeast controls showing interaction and no interaction were provided by the Matchmaker™ GAL4 Two-Hybrid System 3 (Clontech).

Confocal Microscopy

For BiFC and protein subcellular localization assays, an Olympus IX83 confocal microscopy (Japan) was used. The excitation wavelengths used for Venus and GFP were 514 and 488 nm, respectively, and their emissions were detected between 500 to 540 nm. The mCherry fluorescence was excited at 559 nm wavelength and specific emissions between 600 and 680 nm were collected. The subsequent image processing and figure generation were conducted with Olympus Fluoview and Adobe Illustrator.

Accession Numbers

Accession numbers are as follows: AtMKK1, AT4G26070; AtMKK2, AT4G29810; SIMKK1/2, Solyc12g009020; StMKK1, Sotub12g010200; NbMKK1/2, Niben101Scf10103g03014, Niben101Scf00611G07010, Niben101Scf02790g03012, Niben101Scf13387g00027.

Results

***Phytophthora infestans* effector PITG20303 promotes pathogen colonization**

To investigate whether PITG20303 is a virulence effector that promotes *P. infestans* colonization *in planta*, *GFP-PITG20303* and the control *GFP-GUS* were transiently expressed into *Nicotiana benthamiana* leaves and subsequently used for infection assays. The results demonstrate that PITG20303 significantly promotes *P. infestans* colonization at 5 days after inoculation (dai) (Figure 1). To investigate if PITG20303 also promotes other *Phytophthora* pathogen colonization, we inoculated *GFP-PITG20303* and *GFP-GUS* expressed leaves with *Phytophthora parasitica*. The results showed that PITG20303 significantly promotes *P. parasitica* colonization at 3 dai (Supplemental Figure 1). The expression of *GFP-PITG20303* and *GFP-GUS* were confirmed by western blot (Supplemental Figure 1d).

In a previous report PITG20300 was shown to localize to the plasma membrane and partially to the nucleus (Bozkurt et al., 2011), while its virulent allele PITG20303 appeared to localize in the nucleus and the cytoplasm (Zheng et al., 2014). To confirm this, we co-agroinfiltrated *GFP-PITG20303*, *GFP-PITG20300* and the control *GFP* with the plasma membrane marker myr-mCherry (a myristoylation site fused to the N-terminus of mCherry) and the nuclear marker H2B-mCherry (Long et al., 2019) into *N. benthamiana* leaves, respectively. The subcellular localization was examined using confocal microscopy. The results showed that *GFP-PITG20303* was observed in the nucleus and the signals overlapped with H2B-mCherry in the nucleus, some weak signals were also found on the plasma membrane overlapped with myr-mCherry (Supplemental Figure 2). *GFP-PITG20300* localizes mainly on the plasma membrane and weakly in the nucleus, we observed the signals nicely overlapped with myr-mCherry on the plasma

membrane and weakly with H2B-mCherry in the nucleus. Stable expression of the fusion proteins was confirmed by western blot, and the ratios of plasma membrane/nuclear proteins of two effectors were confirmed by isolation of plasma membrane and nuclear proteins (Supplemental Figure 3). The results showed that PITG20303 and PITG20300 all localize to the plasma membrane and nucleus. However, for PITG20303 the proportion of nuclear- and plasma membrane- localized proteins is similar, being about 50% each, while about 80% of PITG20300 is localized on the plasma membrane and only 16% localized inside the nucleus (Supplemental Figure 3). The plasma membrane and nuclear markers show solely localization either on the plasma membrane or inside the nucleus.

To investigate which subcellular localization is required for the virulence activity of PITG20303, we fused a myristoylation site (myr) to the N-terminus of GFP-20303, nuclear export (NES) and nuclear import (NLS) signals to the C-terminus of GFP-20303. We transiently expressed *Myr-GFP-20303*, *GFP-PITG20303NES*, *GFP-PITG20303NLS* in *N. benthamiana* leaves, and confocal microscopy results showed that the myristoylation sites target GFP-20303 to the plasma membrane, the NES signal targets GFP-20303 outside the nucleus, and the NLS signal targets GFP-20303 mainly inside the nucleus as expected (Supplemental Figure 4a). We then tested the functions of *Myr-GFP-20303*, *GFP-PITG20303NES*, and *GFP-PITG20303NLS* in *P. infestans* colonization using detached leaf assays. The results showed that either plasma membrane (myr- or NES- fusion proteins) or nuclear localized PITG20303 (NLS-fusion protein) all promoted *P. infestans* colonization (Supplemental Figure 4b, c, d). The integrity of fusion proteins were shown by western blots in Supplemental Figure 4e.

Both PiPITG20303 and PiPITG20300 target a potato StMKK1 protein

To explore the molecular mechanism of PITG20303 in host defence suppression, we identified its host targets by yeast two hybrid (Y2H) screening. We constructed a prey library from a combination of RNA prepared at 0 and 12 hours after *P. infestans* infection of a compatible tomato cultivar Moneymaker. Using PITG20303 as the bait to screen against this prey library, we identified several PITG20303-interacting candidate proteins. After a one to one Y2H confirmation of interaction, and functional analysis of targets in plant immunity, MKK1 was selected as a candidate target. To confirm the interaction between PITG20303 and MKK1, we cloned the full-length potato *StMKK1* and tomato *SIMKK1* from the potato cultivar Qingshu9 and the tomato cultivar Moneymaker, respectively. A pairwise Y2H assay was performed using PITG20303 as bait and StMKK1 as prey with empty vector as negative control. The results confirmed that both PITG20303 and PITG20300 interacts with StMKK1 and SIMKK1 in yeast cells (Figure 2a; Supplemental Figure 5a). Their *in planta* specific interaction was further confirmed by co-

immunoprecipitation (Co-IP) assays. Results show that both myc-PITG20303 and myc-PITG20300 interact with StMKK1 in Co-IP assays (Figure 2b). We also performed firefly luciferase complementation imaging (LCI) assays to confirm the interaction. The combination of GmBZR2 and PP2C was used as positive control (Lu et al., 2017). The results showed that the combination of StMKK1-nluc with cluc-20303 or cluc-20300, restored the catalytic activity of luciferase even stronger than that of the positive control (Figure 2c, Supplemental Figure 5b). The interaction of NbMKK1 with PITG20303 or PITG20300 were also found in Co-IP assays (Supplemental Figure 5c). To determine the subcellular localization of the PITG20303 and StMKK1 interaction, we performed a bimolecular fluorescence complementation (BiFC) assay. N terminal half YFP (YN) fused *PITG20303* and *PITG20300* were co-agroinfiltrated with C terminal half YFP (YC) fused *StMKK1* into *N. benthamiana* leaves and *YN-PITG04097* and *YN-AVR3a* were co-expressed with *YC-StMKK1* as controls. The results showed that PITG20303 interacts with StMKK1 in the host nucleus, while PITG20300 and the negative controls PITG04097 and AVR3a do not (Figure 2d). The expression of YN- and YC- fusion proteins used in BiFC assays were determined by western blot using appropriate antibodies (Supplemental Figure 5d).

To confirm the subcellular localization of StMKK1 and PITG20303, we performed co-localization assays by co-expressing *GFP-StMKK1* with *mCherry-PITG20303*, *mCherry-PITG20300* and untagged *mCherry*, respectively in *N. benthamiana* leaves. The results showed that mCherry-PITG20300 localizes on the plasma membrane and weakly in the nucleus, while mCherry-20303 localizes in the nucleus and the plasma membrane. The fluorescent of GFP-StMKK1 was predominantly in the cytoplasm and nucleus, and overlapped with free mCherry in the cytoplasm and nucleus and with mCherry-20303 in the nucleus only (Supplemental Figure 6a, 6b). The fluorescent of GFP-StMKK1 weakly overlapped with mCherry-PITG20300 in the nucleus. Taken together, the results showed that both effectors PITG20303 and PITG20300 associates with StMKK1 in the host nucleus, though with different intensities. The expression of GFP-, mCherry- fusion proteins used in co-localization assays were determined by western blot using appropriate antibodies (Supplemental Figure 6c).

***StMKK1* is a negative regulator of plant immunity**

To study the function of *StMKK1* in plant defence to *P. infestans*, we transiently expressed *StMKK1* and control *GFP-GUS* into the right and left panels of *N. benthamiana* leaves, and performed infection assays. The results showed that *StMKK1* expression led to significantly larger lesions compared to the control (Figure 3a, b, c), indicating that *StMKK1* expression promotes susceptibility and it might be targeted by the effector PITG20303 as a susceptibility factor. To further confirm the function of *MKK1*, virus induced gene silencing (VIGS) was set out to reduce

the *MKK1* levels in *N. benthamiana* plants. For selection of target sequence for VIGS, we mined *MKK1* and *MKK2* protein sequences in the Sol genomics network database (<https://solgenomics.net/>), and built a phylogenetic tree of *MKK1/2* protein. Phylogenetic analysis revealed that, in contrast to Arabidopsis, which contains the *MKK1* and *MKK2* genes, in Solanaceous plants, tomato and potato contain one copy of *MKK1*, while *N. benthamiana* has four copies, probably due to its allopolyploid genome (Supplemental Figure 7). The sequence alignment of Nb*MKK1*, SIM*MKK1* and St*MKK1* were shown in Supplemental Figure 8. The alignment of the silencing sequences and the Nb*MKK1* sequences are shown in Supplemental Figure 9. Our construct for VIGS was designed to silence all four copies of the Nb*MKK1* gene. qRT-PCR analysis showed that all 4 copies of Nb*MKK1* genes were efficiently silenced by the TRV-*MKK1* construct, and no obvious developmental phenotype was observed compared to the control (Supplemental Figure 10). TRV-*GUS* and TRV-Nb*MKK1* leaves were harvested for detached leaf assays using *P. infestans* isolate 14-3-GFP. The results showed that TRV-Nb*MKK1* plants developed significantly smaller lesions compared to the control TRV-*GUS* plants (Figure 3d, e, f), further confirming that *MKK1* functions as a negative regulator of plant immunity.

Previous reports show that Arabidopsis *AtMKK1/2* play roles in plant PTI responses. To reveal the role of potato *StMKK1* in plant PTI response, *StMKK1* was transiently expressed in *N. benthamiana* leaves for 2 days before being treated with the bacterial PAMP flg22. The leaves were then harvested 3 hours after flg22 treatment to assess PTI responsive gene expression. The results showed that the expression of *FRK* and *WRKY33* genes were significantly repressed in *StMKK1* expressing leaves compared to the control plants (Figure 3g). Moreover, on *MKK1/2*-silenced *N. benthamiana* plants, upon flg22 treatment the expression of *FRK* and *WRKY33* were induced significantly (Figure 3i) compared to the control, which again indicated its role in regulation of plant early PTI response. Reactive oxygen species (ROS) production was analysed on *MKK1*-overexpressed and -silenced plants. The results showed that on *StMKK1* overexpressed leaves the flg22 triggered ROS production was reduced to about 60% compared to the control *GFP-GUS* leaves (Figure 3h). However, ROS production was increased to nearly 2 times on TRV-*MKK1* plants than the control TRV-*GUS* plants (Figure 3j). These results indicated that *MKK1* negatively regulates plant PTI responses.

The kinase activity of StMKK1 is required for effector interaction and plant immunity repression

To test whether the functional kinase domain of *StMKK1* is necessary for the interaction with the effector PITG20303, we generated two independent mutations that abolish the key residues that are essential for kinase activity of *MKK1*, i.e. the core catalytic arginine (R) and aspartate (D)

of the conserve RD kinase motif were substituted to alanine residues, shown as StMKK1^{AA} (StMKK1^{R191A, D192A}), and the key lysine (K) was substituted to methionine (M), shown as StMKK1^{K99M}. We also generated a constitutively active phospho-mimicking form of StMKK1^{DE} (StMKK1^{T220D, T226E}), via substitution of the conserved Ser/Thr to Asp/Glu residues in the activation loop as described for tobacco and tomato MKK1 (Yang et al., 2001; Li et al., 2014b). Co-IP results showed that the kinase-deficient mutations of StMKK1 lost its ability in interaction with the effector PITG20303 and PITG20300 (Figure 4a, b), while the constitutively active StMKK1^{DE} remained the interaction with PITG20303 and PITG20300 (Figure 4c). Effector PITG04097, AVR1-like and GFP-GUS were used as negative controls. Thus, we conclude that the kinase activity of StMKK1 is necessary for the interaction with PITG20303. We subsequently tested StMKK1^{AA}, StMKK1^{K99M} and StMKK1^{DE} in plant defence against *P. infestans* using transient expression assays. The results showed that except the StMKK1^{DE} all the kinase-deficient mutants lost the ability in promoting *P. infestans* colonization (Figure 4d-e), indicating that StMKK1 requires its kinase activity to promote *P. infestans* infection. The role of StMKK1^{DE} was abolished with an N-terminal GFP tag, thus we used StMKK1^{DE}-myc in the interaction and infection assays. The role of StMKK1, StMKK^{AA} and StMKK1^{K99M} was not affected by N-terminal GFP or C-terminal myc tag. To confirm StMKK1 has self-phosphorylation activities and kinase-deficient mutant StMKK1^{K99M} does not, we performed *in vitro* phosphorylation assays using method as described by Ueno et al. (2015). The results showed that His-StMKK1, but not His-StMKK1^{K99M} and control His-GFP, phosphorylates GST-StMPK4, indicating that StMKK1 has self-phosphorylation activity (Supplemental Figure 11).

PITG20303 suppresses plant PTI responses and this suppression depends on NbMKK1

To investigate if PITG20303 could suppress the plant PTI response, *GFP-GUS* and *GFP-20303* were transiently expressed into the left and right panels of *N. benthamiana* leaves, respectively. At 2 day post agroinfiltration (dpi) the transient expressed leaves were then treated with 10 μ M flg22 for 3 hours before the total RNA were isolated. qRT-PCR results showed that *GFP-20303*-expressing leaf halves show a significant reduction in PTI responsive gene expression when compared to the control leaf halves (Figure 5a). *GFP-GUS* and *GFP-20303*-expressing leaves were treated with 10 μ M flg22 at 2 dpi, and the ROS production was analysed. The results showed that the ROS production was significantly reduced to 50% in *GFP-20303*-expressing leaves compared to the control *GFP-GUS* (Figure 5b). These results indicate that the effector PITG20303 could suppress the plant PTI response. The expression of *GFP-GUS* and *GFP-20303* were shown by western blot in Supplemental Figure 12e.

To investigate if *PITG20303* needs *NbMKK1* to suppress plant PTI response, we checked the effect of PTI induced ROS production by *PITG20303* on the *MKK1* silenced and control plants. GFP and GFP-20303 were transiently expressed into TRV-GUS and TRV-MKK1 plants, and at 2 dpi the leaves were treated with 10 μ M flg22 and the ROS production was analysed. If *PITG20303* depends on *NbMKK1* for suppression of PTI, in TRV-MKK1 plants this suppression of ROS production will be compromised. The results showed that in TRV-GUS plants, ROS production was significantly reduced to 40% in *GFP-20303*-expressing leaves compared to the control *GFP*-expressing plants. However, in TRV-MKK1 plants, the ROS production was reduced to about 70% in *GFP-20303*-expressing leaves compared to the control (Supplemental Figure 12a). This result suggested that effector *PITG20303* may partially depend on *NbMKK1* in the suppression of plant PTI response. Since *PITG20303* showed virulence functions when localized on plasma membrane and nucleus (Supplemental Figure 4), we speculate that the effector may have multiple host targets. *StMKK1* was shown to localize in the cytoplasm and nucleus, we thus hypothesize that the nuclear localized *PITG20303* may largely depend on *StMKK1* for its virulence activity. Thus, we investigated the effect of PTI induced ROS production by *GFP-20303NLS* on TRV-MKK1 plants. The results show that *GFP-20303NLS* suppresses ROS production in TRV-GUS plants to about 40% compared to the control *GFP*. However, in TRV-MKK1 plants, compared to the *GFP* control, *GFP-20303NLS* plants do not suppress flg22 triggered ROS production (Supplemental Figure 12b). The effect of *GFP-20300* and *GFP-20303NLS* were also checked, and we observed that in both TRV-GUS and TRV-MKK1 plants, *GFP-20300* suppresses ROS production to the similar level while *GFP-20300NLS* loses its ability in suppression of ROS in TRV-MKK1 plants (Supplemental Figure 12c, d).

Taken together, these results confirm that the nuclear localized *GFP-20303NLS* and *GFP-20300NLS* depend on *MKK1* for their virulence activity. We further employed VIGS assay to examine if *GFP-20303NLS* and *GFP-20303* requires *NbMKK1* for promoting *P. infestans* colonization. The results showed that in TRV-GUS plants, *GFP-20303NLS* and *GFP-20303* significantly promoted *P. infestans* colonization, as shown by larger lesions. However, in TRV-MKK1 plants, the lesion areas in *GFP*-, *GFP-20303NLS*-expressing sites showed no significant difference, while *GFP-20303*-expressed sites still developed larger lesions (Figure 6). We also find out the nuclear targeted *PITG20300NLS* depends on *MKK1* for promotion of *P. infestans* colonization (Supplemental figure 12h). We thus conclude that only the nuclear localized *PITG20303NLS* and *PITG20300NLS* depend on *NbMKK1* for their full virulence activities. Expression of *NbMKK1* in these assays were shown by qRT-PCR (Supplemental figure 12f). The expression of *GFP*, *GFP-20303*, *GFP-20303NLS*, *GFP-20300* and *GFP-20300NLS* were shown by western blot in Supplemental Figure 12g.

StMKK1 is stabilized by PITG20303 and PITG20300

To test whether the protein accumulation of StMKK1 is altered by effector PITG20303 with and without flg22 treatments, we transiently expressed *GFP-StMKK1* with *myc-20303* and the control *myc-GUS* in the leaves of *N. benthamiana*. Two days after agroinfiltration leaves were harvested for protein isolation. Leaves were treated with 10 μ M flg22 or H₂O 24 hours before harvest. The results showed that in both flg22 treated and untreated leaves, PITG20303 promoted StMKK1 accumulation compared to the control (Figure 7a). To investigate whether PITG20303 stabilized StMKK1 is through the 26S proteasome and if PITG20300 stabilizes StMKK1, *myc-StMKK1* was co-expressed with GFP-20303, GFP-20300 and GFP in *N. benthamiana* leaves. About 36 hours after agroinfiltration, the 26S proteasome inhibitor MG132 or its solvent dimethyl sulfoxide (DMSO) was infiltrated, and 12 hours later leaves were harvested for protein isolation. The results showed that both PITG20303 and PITG20300 promote StMKK1 accumulation in the absence of MG132, while in the presence of MG132 StMKK1 accumulated to the similar levels with and without PITG20303 (Figure 7b). The results indicate that PITG20303 and PITG20300 may increase StMKK1 accumulation through inhibition of 26S proteasome-mediated degradation of StMKK1.

We further performed the plasma membrane and nuclear protein isolation assays. The results showed that StMKK1 is also localized, though weakly, on the plasma membrane. The nuclear StMKK1 is not significantly stabilized by neither PITG20303 nor PITG20300, while the plasma membrane localization of StMKK1 is repressed strongly by PITG20303 and weakly by PITG20300, compared to the control (Supplemental Figure 13). To examine whether PITG20303 alters MAPK activation down stream of StMKK1, we transiently expressed GFP-MPK4 with either *myc-GUS* or *myc-PITG20303* in *N. benthamiana* leaves and checked for activation of MPK4 protein upon flg22 treatment. The results showed that *myc-MPK4*, as well as MPK3/MPK6, are activated upon flg22 treatment, at 10 and 15 minutes post treatment (Supplemental Figure 14). However, PITG20303 does not affect MPK activation as no clear differences were observed on MPK3/6/4 bands between *PITG20303* and *GUS* infiltrated leaves.

Discussion

The virulent variant of AVRblb2, *PITG20303*, was shown to be expressed in *P. infestans* isolates T30-4, 88069, 1306 and Pa21106 during potato infection (Haas et al., 2009; Ah-Fong et al., 2017; Yin et al., 2017), and PITG20303 was secreted as it was found in the secretome of *P. infestans* (Meijer et al., 2014). In this study we demonstrate that PITG20303 localizes to the nucleus and the plasma membrane of the plant to promote pathogen colonization (Figure 1;

Supplemental Figure 1 & 2). PITG20303 and its avirulent variant PITG20300 all interact *in planta* with a potato defence negative regulator StMKK1 protein (Figures 2). The consequence of this interaction is to promote *P. infestans* colonization and suppress PTI responses (Figures 5 and 6). We also provide evidence that PITG20303 and PITG20300 stabilize StMKK1 and the virulence functions of nuclear targeted PITG20303NLS and PITG20300NLS are dependent on StMKK1 (Figure 7; Supplemental Figure 12). There are 7 paralogs of the Avrblb2 family (PITG04085, PITG04086, PITG20301, PITG20303, PITG18683, PITG04090, PITG20300) found in the genome of *P. infestans* T30-4 (Haas et al., 2009), which forms 4 variants and one of the variants in which a Phe residue at position 69 in the protein replaces the Ala/Ile/Val residue, in PITG20301 and PITG20303, resulting in a loss of recognition by its corresponding resistance gene *Rpi-blb2*. PITG20300 was reported to localize to the plasma membrane to target and inhibit the secretion of a host cysteine protease C14 (Bozkurt et al., 2011). The presence of different variants of Avrblb2 in *P. infestans* isolates indicates the importance of AVRblb2 effector family in pathogen virulence. Here we have demonstrated the novel function for Avrblb2 family effector PITG20303 in suppressing PTI immunity via interaction with the StMKK1 protein. Investigating the host target and virulence mechanism of Avrblb2 extends our knowledge of the roles of this important Avrblb2 family in *P. infestans* pathogenicity.

Subcellular localization assays show that PITG20303 and PITG20300 all show a nuclear and plasma membrane localization. However, PITG20303 localizes mainly in the nucleus and nuclear speckles, with weak signals on plasma membrane, while PITG20300 localizes more on the plasma membrane, with weak signals in the nucleus and with no nuclear speckles found (Supplemental Figure 2). The plasma membrane/nuclear protein isolation assays further showed that for PITG20303 the proportion of nuclear- and plasma membrane- localized proteins is similar, being about 50% each. About 80% of PITG20300 is localized on the plasma membrane and only 16% localized inside the nucleus (Supplemental Figures 2 and 3). Co-localization of these two effectors with StMKK1 showed that PITG20303 nicely co-localizes with StMKK1 in the nucleus, while PITG20300 weakly co-localizes with StMKK1 in the nucleus (Supplemental Figure 6). Both effectors were shown to interact with StMKK1 in Y2H, Co-IP and LCI assays (Figure 2; Supplemental Figure 5). By BiFC assays, PITG20303 interacts with StMKK1 in the nucleus, and the interaction was not observed for PITG20300 (Figure 2). Since BIFC assay for PITG20303 and StMKK1 showed an interaction only in the host nucleus, it is likely the plasma membrane interaction is not sufficient to be detected by BIFC. PITG20300 localizes less in the nucleus than PITG20303 (Supplemental Figure 2 & 3), thus the interaction of PITG20300 and StMKK1 is likely weaker than PITG20303 and StMKK1, leading to a failure of interaction detected by BiFC assay.

The fact that GFP-20303 and the nuclear targeted GFP-20303NLS/GFP-20300NLS partially or completely depends on NbMKK1 for suppression of ROS production and enhancement of infection while PITG20300 does not (Figure 6 & Supplemental Figure 12), indicates that the nuclear localization of both effectors utilizes this interaction to repress plant PTI. PITG20303 likely have other host target proteins on the plasma membrane like PITG20300, as the plasma membrane localized myr-PITG20303 promotes pathogen colonization. Taken together, our results suggest that both PITG20303 and PITG20300 are likely target multiple host proteins to modulate plant immunity. It is possible that they target plasma membrane related proteins. This is similar to the *P. infestans* effector AVR3a, which was found to target and stabilize the E3-ligase CMPG1 (Bos et al., 2010) and the cinnamyl alcohol dehydrogenase CAD7 (Li et al., 2019).

Our results presented here demonstrate that StMKK1 negatively regulates plant immunity to the late blight disease *P. infestans* by repressing plant PTI responses (Figure 3). The role of MPK cascade proteins in plant immunity is rather complicated. For example, MEKK1-MKK1/2-MPK4 cascade proteins were reported as both positive (Zhang et al., 2017) and negative regulators of plant defense. For example, cotton *GhMKK1* enhances plant susceptibility to the bacterial pathogen *Ralstonia solanacearum* (Lu et al., 2013). Thus, we think StMKK1 might have additional roles in repressing plant immunity other than participating in MEKK1-MKK1/2-MPK4 cascade. It may participate in plant hormone biosynthesis or signaling pathways, as several MAPK cascade proteins were found to participate in SA signaling (Jagodzik et al., 2018).

The constitutively activated StMKK1^{DE} interacts with both effectors and promotes pathogen colonization, while the kinase-deficient mutant StMKK1^{K99M} and StMKK1^{AA} lost this ability (Figure 4), indicating that the kinase activity of StMKK1 is required for PITG20303 interaction and plant defense repression. We also showed that without phosphorylation by the upstream kinase, StMKK1, but not StMKK1^{K99M}, phosphorylates StMPK4 (Supplemental Figure 11), suggesting that StMKK1 has self-phosphorylation activity and confirming that StMKK1 kinase activity is essential for effector interaction.

MAPK cascades play essential roles in plant immunity, especially in plant PTI responses. Successful plant pathogens secrete intracellular effectors to directly target MAPK cascade proteins to interfere with PTI (Teper et al., 2018; Hu et al., 2019; Eschen-Lippold et al., 2016). Most of the effectors that target MAPK cascade components show a biochemical activity in regulating MAPK kinase activity. In *Arabidopsis* the *mkk1/2* shows autoimmune phenotype mediated by the activation of a plant NB-LRR protein SUMM2, which senses the integrity of the MEKK1-MKK1/2-MPK4 cascade (Zhang et al., 2012; 2017). Thus, interference of the MEKK1-MKK1/2-MPK4 cascade by pathogen effectors leads to the activation of SUMM2-mediated plant immunity, and that was true for *P. syringae* effector HopAI1 which inactivates MPK4 and triggers

immunity when expressed in plants (Zhang et al., 2012). In our case, although PITG20303 targets StMKK1, it neither triggered HR or autoimmunity in *N. benthamiana* nor disturbed flg22-triggered MPK4 phosphorylation (Supplemental Figure 14). This indicates that PITG20303 does not disturb the MEKK1-MKK1/2-MPK4 kinase cascade, thus it does not trigger a SUMM2-mediated defense response. It is also possible that SUMM2 is missed in *N. benthamiana* plants.

PITG20303 suppresses plant immunity, as measured by *FRK* and *WRKY33* expression and ROS burst (Figure 5), which is negatively regulated by its *in planta* interacting protein StMKK1. This indicates that *StMKK1* functions as a susceptibility gene that is targeted and modulated by the *P. infestans* effector PITG20303. However, how PITG20303 modulates StMKK1 is not fully clear. Here we showed that over-expression of the effector PITG20303 and PITG20300 could stabilize the co-expressed StMKK1 protein. Further investigation on the effect of PITG20303 and PITG20300 on StMKK1 auto-phosphorylation or identifying and testing the effect of PITG20303 on the phosphorylation of StMKK1 substrate proteins in suppression of plant immunity may help us answering this question.

In summary, we show the AVRblb2 family effector PITG20303 and PITG20300 target and stabilize a nuclear and cytoplasmic localized StMKK1 protein, and perturbs plant PTI responses that were negatively regulated by StMKK1 (Figure 8). Furthermore, we uncovered a role of StMKK1 in negative regulation of PTI responses by repressing the expression of *FRK* and *WRKY33* and ROS production. The kinase activity of StMKK1 is required for its repression of PTI, indicating it might have additional substrates *in planta* which is involved in plant immunity suppression. This research provides evidences that oomycete RXLR effectors can directly target a MAPK cascade protein and use it as a susceptibility gene to interfere with plant immunity. Our findings may lead to identifying novel plant susceptibility genes, and these knowledge can help improving plant resistance to *Phytophthora* pathogens.

AUTHOR CONTRIBUTIONS

Y.D., Y.M., and W.S. designed the research. Y.G., Y.D., X.C., X.Z., H.Z., Y.M., G.H. and F.L. performed the experiments. Y.G. and Y.D. screened the yeast-two-hybrid library. Y.D. and X.C. analysed the data. Y.D. and W.S. wrote the manuscript with contribution from all authors. YD, XC and YG contributed equally to this work.

ACKNOWLEDGEMENTS

We thank Dr. Brett Tyler (Oregon State University, USA), Jim Beynon (Warwick University, UK) for useful discussions and advices, and Northwest A&F University Life Science Research Core Services for providing advanced facilities. This work was supported by the National Natural

Science Foundation of China (31701770 and 31561143007), China Agriculture Research System (CARS-09), the Postdoctoral Science Foundation (2016M600818, 2019T120956 and 2017BSHYDZZ63), Northwest A&F University Scientific Research Fund for Advanced Talents and Young Talent Training Program (2452018028 and 2452017069), the Shaanxi Province Science and Technology Fund (2017JQ3013), and the Project 111 from the State Administration of Foreign Experts Affairs (#B18042).

References

- Ah Fong, AMV, Kim, KS, Judelson, HS. 2017.** RNA-seq of life stages of the oomycete *Phytophthora infestans* reveals dynamic changes in metabolic, signal transduction, and pathogenesis genes and a major role for calcium signaling in development. *BMC Genomics* 18: 198.
- Berriri, S, Garcia, AV, Frei dit Frey, N, Rozhon, W, Pateyron, S, Leonhardt, N, Montillet, JL, Leung, J, Hirt, H, and Colcombet, J. 2012.** Constitutively active Mitogen-activated protein kinase versions reveal functions of *Arabidopsis* MPK4 in pathogen defense signaling. *The Plant Cell* 24: 4281-4293.
- Bi, G, and Zhou, JM. 2017.** MAP kinase signaling pathways: a hub of plant-microbe interactions. *Cell Host & Microbe* 21: 270-273.
- Boevink, PC, Wang, X, McLellan, H, He, Q, Naqvi, S, Armstrong, MR, Zhang, W, Hein, I, Gilroy, EM, Tian, Z, et al. 2016.** A *Phytophthora infestans* RXLR effector targets plant PP1c isoforms that promote late blight disease. *Nature Communications* 7: 10311.
- Bos, JI, Armstrong, MR, Gilroy, EM, Boevink, PC, Hein, I, Taylor, RM, Zhendong, T, Engelhardt, S, Vetukuri, RR, Harrower, B, et al. 2010.** *Phytophthora infestans* effector AVR3a is essential for virulence and manipulates plant immunity by stabilizing host E3 ligase CMPG1. *Proceedings of the National Academy of Sciences USA* 107: 9909-9914.
- Bozkurt, TO, Schornack, S, Win, J, Shindo, T, Ilyas, M, Oliva, R, Cano, LM, Jones, AM, Huitema, E, van der Hoorn, RA, et al. 2011.** *Phytophthora infestans* effector AVRblb2 prevents secretion of a plant immune protease at the haustorial interface. *Proceedings of the National Academy of Sciences USA* 108: 20832-20837.
- Bouwmeester, K, de Sain, M, Weide, R, Gouget, A, Klamer, S, Canut, H, and Govers, F. 2011.** The lectin receptor kinase LecRK-I.9 is a novel *Phytophthora* resistance component and a potential host target for a RXLR effector. *PLoS Pathogens* 7: e1001327.
- Champouret, N, Bouwmeester, K, Rietman, H, van der Lee, T, Maliepaard, C, Heupink, A, van de Vondervoort, PJ, Jacobsen, E, Visser, RG, van der Vossen, EA, et al. 2009.** *Phytophthora infestans* isolates lacking class I *ipiO* variants are virulent on *Rpi-blb1* potato. *Molecular Plant-Microbe Interactions* 22: 1535-1545.

- Cui, HT, Wang, YJ, Xue, L, Chu, JF, Yan, CY, Fu, JH, Chen, MS, Innes, RW, and Zhou, JM. 2010. *Pseudomonas syringae* effector protein AvrB perturbs *Arabidopsis* hormone signaling by activating MAP kinase 4. *Cell Host & Microbe* 7: 164-175.
- Chen, H, Zou, Y, Shang, Y, Lin, H, Wang, Y, Cai, R, Tang, X, Zhou, J M. 2008. Firefly luciferase complementation imaging assay for protein-protein interactions in plants. *Plant Physiology* 146: 368-76.
- Cheng, BP, Yu, XL, Ma, ZC, Dong, SM, Dou, DL, Wang, YC, and Zheng, XB. 2012. *Phytophthora sojae* effector Avh331 suppresses the plant defence response by disturbing the MAPK signalling pathway. *Physiological and Molecular Plant Pathology* 77: 1-9.
- Dagdas, YF, Belhaj, K, Maqbool, A, Chaparro-Garcia, A, Pandey, P, Petre, B, Tabassum, N, Cruz-Mireles, N, Hughes, RK, Sklenar, J, et al. 2016. An effector of the Irish potato famine pathogen antagonizes a host autophagy cargo receptor. *eLife* 5: e10856.
- Du, Y, Mpina, MH, Birch, PR, Bouwmeester, K, and Govers, F. 2015a. *Phytophthora infestans* RXLR effector AVR1 interacts with exocyst component Sec5 to manipulate plant immunity. *Plant Physiology* 169: 1975-1990.
- Du, Y, Berg, J, Govers, F, and Bouwmeester, K. 2015b. Immune activation mediated by the late blight resistance protein R1 requires nuclear localization of R1 and the effector AVR1. *New Phytologist* 207: 735-747.
- Eschen-Lippold, L, Jiang, XY, Elmore, JM, Mackey, D, Shan, LB, Coaker, G, Scheel, D, and Lee, J. 2016. Bacterial AvrRpt2-Like cysteine proteases block activation of the *Arabidopsis* Mitogen-activated protein kinases, MPK4 and MPK11. *Plant Physiology* 171: 2223-2238.
- Fan, G, Yang, Y, Li, T, Lu, W, Du, Y, Qiang, X, Wen, Q, and Shan, W. 2018. A *Phytophthora capsici* RXLR effector targets and inhibits a plant PPlase to suppress endoplasmic reticulum-mediated immunity. *Molecular Plant* 11: 1067-1083.
- Feng, F, Yang, F, Rong, W, Wu, X, Zhang, J, Chen, S, He, C, and Zhou, JM. 2012. A *Xanthomonas* uridine 5'-monophosphate transferase inhibits plant immune kinases. *Nature* 485: 114-118.
- Haas, BJ, Kamoun, S, Zody, MC, Jiang, RHY, Handsaker, RE, Cano, LM, Grabherr, M, Kodira, CD, Raffaele, S, Torto-Alalibo, T, et al. 2009. Genome sequence and analysis of the Irish potato famine pathogen *Phytophthora infestans*. *Nature* 461: 393-398
- Hardham, AR, and Cahill, DM. 2010. The role of oomycete effectors in plant-pathogen interactions. *Functional Plant Biology* 37: 919-925.
- Haverkort, AJ, Boonekamp, PM, Hutten, R, Jacobsen, E, Lotz, LAP, Kessel, GJT, Vossen, JH, and Visser, RGF. 2016. Durable late blight resistance in potato through dynamic varieties obtained by cisgenesis: Scientific and Societal Advances in the DuRPh Project. *Potato Research* 59: 35-66.
- He, P, Shan, L, Lin, NC, Martin, GB, Kemmerling, B, Nurnberger, T, and Sheen, J. 2006. Specific bacterial suppressors of MAMP signaling upstream of MAPKKK in *Arabidopsis* innate immunity. *Cell* 125: 563-575.

- He, Q, Naqvi, S, McLellan, H, Boevink, PC, Champouret, N, Hein, I, and Birch, PRJ. 2018. Plant pathogen effector utilizes host susceptibility factor NRL1 to degrade the immune regulator SWAP70. *Proceedings of the National Academy of Sciences USA* 115: E7834-E7843.
- Hu, T, Huang, C, He, Y, Castillo-Gonzalez, C, Gui, X, Wang, Y, Zhang, X, and Zhou, X. 2019. β C1 protein encoded in geminivirus satellite concertedly targets MKK2 and MPK4 to counter host defense. *PLoS Pathogens* 15: e1007728.
- Jagodzik, P, Tajdel-Zielinska, M, Ciesla, A, Marczak, M, Ludwikow, A. 2018. Mitogen-Activated Protein Kinase Cascades in Plant Hormone Signaling. *Frontiers in Plant Science* 9: 1387.
- Ingle, RA, Carstens, M, and Denby, KJ. 2006. PAMP recognition and the plant-pathogen arms race. *BioEssays* 28: 880-889.
- Jones, JDG, and Dangl, JL. 2006. The plant immune system. *Nature* 444: 323-329.
- Kale, SD., Gu, B., Capelluto, DGS, Dou, D, Feldman, E, Rumore, A, Arredondo, FD, Hanlon, R, Fudal, I, Rouxel, T, Lawrence, CB, Shan, WX, and Tyler, BM. 2010. External lipid PI3P mediates entry of eukaryotic pathogen effectors into plant and animal host cells. *Cell* 142: 284-295.
- King, SR, McLellan, H, Boevink, PC, Armstrong, MR, Bukharova, T, Sukarta, O, Win, J, Kamoun, S, Birch, PR and Banfield, MJ. 2014. *Phytophthora infestans* RXLR effector PexRD2 interacts with host MAPKKK epsilon to suppress plant immune signaling. *The Plant Cell* 26: 1345-1359.
- Kong, L, Qiu, XF, Kang, JG, Wang, Y, Chen, H, Huang, J, Qiu, M, Zhao, Y, Kong, GH, Ma, ZC, et al. 2017. A *Phytophthora* effector manipulates host histone acetylation and reprograms defense gene expression to promote infection. *Current Biology* 27: 981-991.
- Kong, Q, Qu, N, Gao, MH, Zhang, ZB, Ding, XJ, Yang, F, Li, YZ, Dong, OX, Chen, S, Li, X, et al. 2012. The MEKK1-MKK1/MKK2-MPK4 kinase cascade negatively regulates immunity mediated by a Mitogen-activated protein kinase kinase kinase in *Arabidopsis*. *The Plant Cell* 24: 2225-2236.
- Li, B, Jiang, S, Yu, X, Cheng, C, Chen, S, Cheng, Y, Yuan, JS, Jiang, D, He, P, and Shan, L. 2015. Phosphorylation of trihelix transcriptional repressor ASR3 by MAP KINASE4 negatively regulates *Arabidopsis* immunity. *The Plant Cell* 27: 839-856.
- Li, L, Kim, P, Yu, L, Cai, G, Chen, S, Alfano, JR, and Zhou, JM. 2016. Activation-dependent destruction of a co-receptor by a *Pseudomonas syringae* effector dampens plant immunity. *Cell Host & Microbe* 20: 504-514.
- Li, L, Li, M, Yu, L, Zhou, Z, Liang, X, Liu, Z, Cai, G, Gao, L, Zhang, X, Wang, Y, et al. 2014a. The FLS2-associated kinase BIK1 directly phosphorylates the NADPH oxidase RbohD to control plant immunity. *Cell Host & Microbe* 15: 329-338.
- Li, X, Zhang, Y, Huang, L, Ouyang, Z, Hong, Y, Zhang, H, Li, D, and Song, F. 2014b. Tomato SIMKK2 and SIMKK4 contribute to disease resistance against *Botrytis cinerea*. *BMC Plant Biology* 14: 166.
- Ling, TF, Bellin, D, Vandelle, E, Imanifard, Z, and Delledonne, M. 2017. Host-mediated S-Nitrosylation disarms the bacterial effector HopA11 to reestablish immunity. *The Plant Cell* 29: 2871-2881.

- Li, T, Wang, Q, Feng, R, Li, L, Ding, L, Fan, G, Li, W, Du, Y, Zhang M, et al. 2019. Negative regulators of plant immunity derived from cinnamyl alcohol dehydrogenases are targeted by multiple *Phytophthora* Avr3a-like effectors. *New Phytologist*. 10.1111/nph.16139.
- Long, Y, Xie, D, Zhao, Y, Shi, D, and Yang, W. 2019. BICELLULAR POLLEN 1 is a modulator of DNA replication and pollen development in *Arabidopsis*. *New Phytologist*, 222: 588-603.
- Lu, W, Chu, X, Li, Y, Wang, C, and Guo, X. 2013. Cotton GhMKK1 induces the tolerance of salt and drought stress, and mediates defence responses to pathogen infection in transgenic *Nicotiana benthamiana*. *PLoS ONE* 8: e68503.
- Lu, X, Xiong, Q, Cheng, T, Li, QT, Liu, XL, Bi, YD, Li, W, Zhang, WK, Ma, B, Lai, YC, et al. 2017. A PP2C-1 allele underlying a quantitative trait locus enhances Soybean 100-seed weight. *Molecular Plant* 10: 670-684.
- Meijer, HJG, Mancuso, FM, Espadas, G, Seidl, MF, Chiva, C, Govers, F, and Sabido, E. 2014. Profiling the Secretome and Extracellular Proteome of the Potato Late Blight Pathogen *Phytophthora infestans*. *Molecular & Cellular Proteomics* 13: 2101-2113.
- McLellan, H, Boevink, PC, Armstrong, MR, Pritchard, L, Gomez, S, Morales, J, Whisson, SC, Beynon, JL, and Birch, PR. 2013. An RXLR effector from *Phytophthora infestans* prevents re-localisation of two plant NAC transcription factors from the endoplasmic reticulum to the nucleus. *PLoS Pathogens* 9: e1003670.
- Murphy, F, He, Q, Armstrong, M, Giuliani, LM, Boevink, PC, Zhang, W, Tian, Z, Birch, PRJ, and Gilroy, EM. 2018. The potato MAP3K StVIK is required for the *Phytophthora infestans* RXLR effector Pi17316 to promote disease. *Plant Physiology* 177: 398-410.
- Oh, S-K, Young, C, Lee, M, Oliva, R, Bozkurt, TO, Cano, LM, Win, J, Bos, JI, Liu, HY, van Damme, M, Morgan, W, Choi, D, Van der Vossen, EA, Vleeshouwers, VG, and Kamoun, S, et al. 2009. In planta expression screens of *Phytophthora infestans* RXLR effectors reveal diverse phenotypes, including activation of the *Solanum bulbocastanum* disease resistance protein Rpi-blb2. *The Plant Cell* 21: 2928–2947.
- Oliva, RF, Cano, LM, Raffaele, S, Win, J, Bozkurt, TO, Belhaj, K, Oh, SK, Thines, M, and Kamoun, S. 2015. A recent expansion of the RXLR effector gene *Avrblb2* is maintained in global populations of *Phytophthora infestans* indicating different contributions to virulence. *Molecular Plant-Microbe Interactions* 28: 901-912.
- Qiao, Y, Shi, J, Zhai, Y, Hou, Y, and Ma, W. 2015. *Phytophthora* effector targets a novel component of small RNA pathway in plants to promote infection. *Proceedings of the National Academy of Sciences USA* 112: 5850-5855.
- Ren, Y, Armstrong, M, Qi, Y, McLellan, H, Zhong, C, Du, B, Birch, PRJ, and Tian, Z. 2019. *Phytophthora infestans* RXLR effectors target parallel steps in an immune signal transduction pathway. *Plant Physiology* 180: 2227-2239.
- Saunders, DGO, Breen, S, Win, J, Schornack, S, Hein, I, Bozkurt, TO, Champouret, N, Vleeshouwers, VGAA, Birch, PRJ, Gilroy, EM, et al. 2012. Host protein BSL1 associates with *Phytophthora*

infestans RXLR effector AVR2 and the *Solanum demissum* immune receptor R2 to mediate disease resistance. The Plant Cell 24: 3420-3434.

Tameling, WIL, and Baulcombe, DC. 2007. Physical association of the NB-LRR resistance protein Rx with a Ran GTPase-activating protein is required for extreme resistance to Potato virus X. The Plant Cell 19: 1682-1694.

Teper, D, Girija, AM, Bosis, E, Popov, G, Savidor, A, and Sessa, G. 2018. The *Xanthomonas euvesicatoria* type III effector XopAU is an active protein kinase that manipulates plant MAP kinase signaling. PLoS Pathogens 14: e1006880.

Tomczynska, I, Stumpe, M, and Mauch, F. 2018b. A conserved RXLR effector interacts with host RABA-type GTPases to inhibit vesicle-mediated secretion of antimicrobial proteins. The Plant Journal 95: 187-203.

Turnbull, D, Yang, L, Naqvi, S, Breen, S, Welsh, L, Stephens, J, Morris, J, Boevink, PC, Hedley, PE, Zhan, J, et al. 2017. RXLR effector AVR2 up-regulates a brassinosteroid responsive bHLH transcription factor to suppress immunity. Plant Physiology 174: 356-369.

Ueno, Y, Yoshida, R, Kishi-Kaboshi, M, Matsushita, A, Jiang, CJ, Goto, S, Takahashi, A, Hirochika, H, & Takatsuji, H. 2015. Abiotic stresses antagonize the rice defence pathway through the Tyrosine-dephosphorylation of OsMPK6. PLoS Pathogens 11: e1005231.

Vetukuri, RR, Whisson, SC, and Grenville-Briggs, LJ. 2017. *Phytophthora infestans* effector Pi14054 is a novel candidate suppressor of host silencing mechanisms. European Journal of Plant Pathology 149: 771-777.

Vleeshouwers, VGAA, Raffaele, S, Vossen, JH, Champouret, N, Oliva, R, Segretin, ME, Rietman, H, Cano, LM, Lokossou, A, Kessel, G, et al. 2011. Understanding and exploiting late blight resistance in the age of effectors. Annual Review of Phytopathology 49: 507-531

Wang, YJ, Li, JF, Hou, SG, Wang, XW, Li, YA, Ren, DT, Chen, S, Tang, XY, and Zhou, JM. 2010. A *Pseudomonas syringae* ADP-Ribosyltransferase inhibits *Arabidopsis* Mitogen-activated protein kinase kinases. The Plant Cell 22: 2033-2044.

Wang, X, Boevink, P, McLellan, H, Armstrong, M, Bukharova, T, Qin, Z, and Birch, PR. 2015. A host KH RNA-binding protein is a susceptibility factor targeted by an RXLR effector to promote late blight disease. Molecular Plant 8: 1385-1395.

Yang KY, Liu YD, Zhang SQ. 2001. Activation of a mitogen-activated protein kinase pathway is involved in disease resistance in tobacco. Proceedings of the National Academy of Sciences USA 98: 741-746.

Yang, L, McLellan, H, Naqvi, S, He, Q, Boevink, PC, Armstrong, M, Giuliani, LM, Zhang, W, Tian, Z, Zhan, J, et al. 2016. Potato NPH3/RPT2-like protein StNRL1, targeted by a *Phytophthora infestans* RXLR effector, is a susceptibility factor. Plant Physiology 171: 645-657.

Yin, JL, Gu, B, Huang, GY, Tian, Y, Quan, JL, Lindqvist-Kreuze, H, Shan, WX. 2017. Conserved RXLR effector genes of *Phytophthora infestans* expressed at the early stage of potato infection are suppressive to host defense. Frontiers in Plant Science 8: 2155.

- Zhang, J, Li, W, Xiang, T, Liu, Z, Laluk, K, Ding, X, Zou, Y, Gao, M, Zhang, X, Chen, S, et al. 2010. Receptor-like cytoplasmic kinases integrate signaling from multiple plant immune receptors and are targeted by a *Pseudomonas syringae* effector. *Cell Host & Microbe* 7: 290-301.
- Zhang, J, Shao, F, Li, Y, Cui, H, Chen, L, Li, H, Zou, Y, Long, C, Lan, L, Chai, J, et al. 2007. A *Pseudomonas syringae* effector inactivates MAPKs to suppress PAMP-induced immunity in plants. *Cell Host & Microbe* 1: 175-185.
- Zhang, ZB, Liu, YN, Huang, H, Gao, MH, Wu, D, Kong, Q, and Zhang, YL. 2017. The NLR protein SUMM2 senses the disruption of an immune signaling MAP kinase cascade via CRCK3. *EMBO Reports* 18: 292-302.
- Zhang, Z, Wu, Y, Gao, M, Zhang, J, Kong, Q, Liu, Y, Ba, H, Zhou, J, and Zhang, Y. 2012. Disruption of PAMP-induced MAP kinase cascade by a *Pseudomonas syringae* effector activates plant immunity mediated by the NB-LRR protein SUMM2. *Cell Host & Microbe* 11: 253-263.
- Zheng, X, McLellan, H, Fraiture, M, Liu, X, Boevink, PC, Gilroy, EM, Chen, Y, Kandel, K, Sessa, G, Birch, PR, et al. 2014. Functionally redundant RXLR effectors from *Phytophthora infestans* act at different steps to suppress early flg22-triggered immunity. *PLoS pathogens* 10: e1004057.
- Zheng, X, Wagener, N, McLellan, H, Boevink, PC, Hua, C, Birch, PRJ, and Brunner, F. 2018. *Phytophthora infestans* RXLR effector SFI5 requires association with calmodulin for PTI/MTI suppressing activity. *New Phytologist* 219: 1433-1446.
- Zhou, J, Wu, S, Chen, X, Liu, C, Sheen, J, Shan, L, and He, P. 2014. The *Pseudomonas syringae* effector HopF2 suppresses *Arabidopsis* immunity by targeting BAK1. *The Plant Journal* 77: 235-245.
- Zipfel, C. 2008. Pattern-recognition receptors in plant innate immunity. *Current Opinion in Immunology* 20: 10-16.

Supplemental information

Supplemental Table 1. Primers used in this study.

Supplemental Figure 1. PITG20303 promotes plant susceptibility to *Phytophthora parasitica*.

Supplemental Figure 2. Subcellular localization of PITG20303 and PITG20300.

Supplemental Figure 3. Plasma membrane and nuclear protein isolation assays.

Supplemental Figure 4. *PITG20303* promotes *P. infestans* colonization at different subcellular localizations.

Supplemental Figure 5. Both *PITG20303* and *PITG20300* interact with StMKK1 and SIMKK1.

Supplemental Figure 6. StMKK1 co-localizes with the effector *PITG20303* in the nucleus of the plant cells.

Supplemental Figure 7. Phylogenetic tree of MKK1/2 proteins from Arabidopsis, rice, populus, tomato, potato and *N. benthamiana*.

Supplemental Figure 8. Sequence alignment of MKK1 from *N. benthamiana*, tomato, and potato.

Supplemental Figure 9. Sequence alignment of TRV-*MKK1* and *NbMKK1* genes.

Supplemental Figure 10. Silencing efficiency and plant morphology of *N. benthamiana* plants inoculated with TRV-*MKK1*.

Supplemental Figure 11. The *in vitro* phosphorylation assays.

Supplemental Figure 12. *NbMKK1* is required for virulence activities of GFP-*PITG20303NLS* and GFP-*PITG20300NLS*.

Supplemental Figure 13. The plasma membrane localized StMKK1 was reduced by *PITG20303* and *PITG20300*.

Supplemental Figure 14. Western blots showing the effect of *PITG20303* on MAPK kinase activities.

Figure legends

Figure 1. Transient expression of *P. infestans* RXLR effector Avrblb2 variant *PITG20303* in *Nicotiana benthamiana* promotes plant susceptibility to *Phytophthora infestans*. a, *Agrobacterium tumefaciens* cells carrying control *GFP-GUS* were infiltrated into the left panel of the leaf, while

the *GFP-PITG20303* were infiltrated into the right panel of the same leaf. Zoospores of *P. infestans* isolate 14-3-GFP were inoculated onto the agroinfiltrated leaves at 1 day post infiltration (dpi), and lesion diameters were measured and lesion areas were scored at 5 day after infection (dai). The bars show the mean lesion areas in mm². Error bars show SE from 12 replicates. Asterisks indicate significant differences ($n \geq 12$; one-sided Student's t-test, $P \leq 0.01$). b, Lesion development was photographed at 5 dai, and lesion areas were indicated with dotted circles. c, Trypan blue staining of the lesions. The experiments were repeated more than three times with similar results.

Figure 2. PITG20303 targets a potato StMKK1 protein. a, Yeast co-expressing PITG20303 and StMKK1 were grown on SD-LW medium and yielded α -galactosidase activity while the empty vector control (EV) with StMKK1 did not. b, Co-immunoprecipitation (Co-IP) was performed using GFP-Trap confirmed that GFP-tagged StMKK1 associated with myc-20303 and myc-20300, but not with the myc-04097 control. +, indicated the expression of proteins in the leaves. Protein loading is indicated by Ponceau stain (Ponceau S). c, The leaf picture on the left shows the infiltration of constructs used in the luciferase complementation assays. The fluorescence signal on the right picture shows the protein-protein interaction. The combination of GmBZR2-nluc with cluc-PP2c was used as positive control. d, BiFC assay confirms that PITG20303 interacts with StMKK1 in the nucleus of the plant. We fused C-terminus of YFP (YC) to the N-terminus of StMKK1, and the N-terminus of YFP (YN) to the N terminus of PITG20303, PITG04097, PITG20300 and AVR3a. YC-StMKK1 was co-agroinfiltrated with YN-20303, YN-04097, YN-20300 and YN-AVR3a into *N. benthamiana* leaves for 2 days before confocal images were taken. Bars indicates 20 μ m.

Figure 3. *StMKK1* negatively regulates plant defence. Average lesion areas in mm² on sites expressing either GFP-GUS or GFP-StMKK1 (a), or on TRV-GUS and TRV-MKK1 VIGS plants (d) were measured and calculated at 5 dai. Zoospores from *P. infestans* isolate 14-3-GFP were used for inoculation. Error bars show SE from more than 10 replicates. Asterisks indicate significant differences ($n \geq 10$; one-sided Student's t-test, $P \leq 0.01$). The experiments were repeated four times with similar results. Representative images of GFP-GUS and GFP-StMKK1 expressed leaves with *P. infestans* lesions before (b) and after (c) trypan blue staining. Representative images of *P. infestans* lesions on TRV-GUS (e) and TRV-MKK1 (f) silenced leaves. qRT-PCR data showing relative expression of the PTI marker genes *FRK* and *WRKY33* in *GFP-GUS*, *GFP-StMKK1* overexpressed leaves (g) and in TRV-GUS, TRV-MKK silenced plant leaves (i). *N. benthamiana* actin gene expression was used for normalization in qRT-PCR assays.

FRK and *WRKY33* gene expression levels in *GFP-GUS* or in *TRV-GUS* plants were set to one. Flg22-induced ROS productions in *StMKK1*-overexpressed (h) and *NbMKK1*-silenced plants (j) were analysed. Leaves were treated with 10 μ M flg22 before ROS production was measured. RUL, relative luminescence units.

Figure 4. The kinase activity of *StMKK1* is required for its interaction with PITG20303 and promotion of *P. infestans* colonization. a-c, Co-immunoprecipitation (Co-IP) was performed using GFP-Trap showed that GFP-tagged *StMKK1*^{AA} (a) and *StMKK1*^{K99M} (b) do not associate with myc-20303. c, *StMKK1*^{DE}-myc associated with GFP-20303 but not with the GFP-GUS control. +, indicated the expression of proteins in the leaves. Protein loading is indicated by Ponceau stain (Ponceau S). d-e, GFP- *StMKK1*^{AA}, GFP-*StMKK1*^{K99M} or *StMKK1*^{DE}-myc were agroinfiltrated together with control GFP-GUS or myc-GUS into *N. benthamiana* leaves as indicated in the pictures. Zoospores of *P. infestans* isolate 14-3-GFP were inoculated onto the agroinfiltrated leaves at 1 days post infiltration (dpi), and lesion diameters were measured at 5 dai. d, The bar graphs showing the mean lesion areas in mm². Error bars show SE from 12 replicates. Asterisks indicate significant differences ($n \geq 12$; one-sided Student's t-test, $P \leq 0.01$). e, Pictures were taken under blue light showing the lesion developments at 5 dai. Lesion areas were indicated with dotted circle. The experiments were repeated more than three times with similar results.

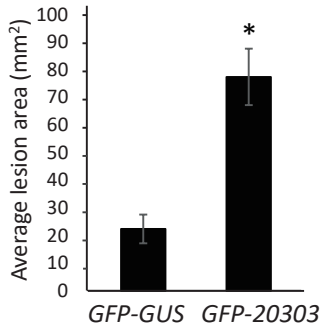
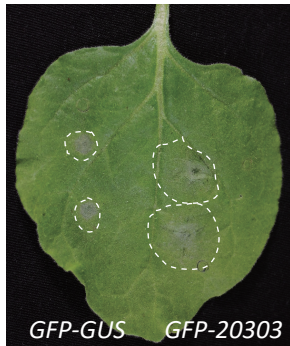
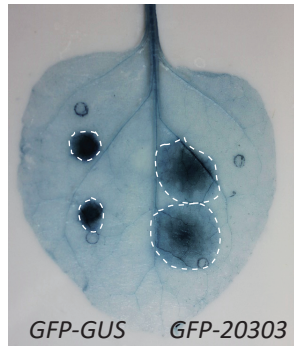
Figure 5. The PITG20303 suppresses plant PTI response. a, qRT-PCR data showing relative expression of PTI maker genes *FRK* and *WRKY33* in *GFP-GUS* and *GFP-20303* overexpressed leaves. The *N. benthamiana* actin gene expression was used for normalization in qRT-PCR assays. The relative expression of *FRK* and *WRKY33* were shown in Y-axis, and gene expression levels in *GFP-20303* were relevant to that in *GFP-GUS* plants. b, ROS production was measured in *PITG20303* and *GFP-GUS* overexpressed leaves after flg22 treatments. Leaves were treated with 10 μ M flg22 before ROS production was measured. RUL, relative luminescence units. The experiments were repeated three times with similar results. Error bars show SE from three technical replicates.

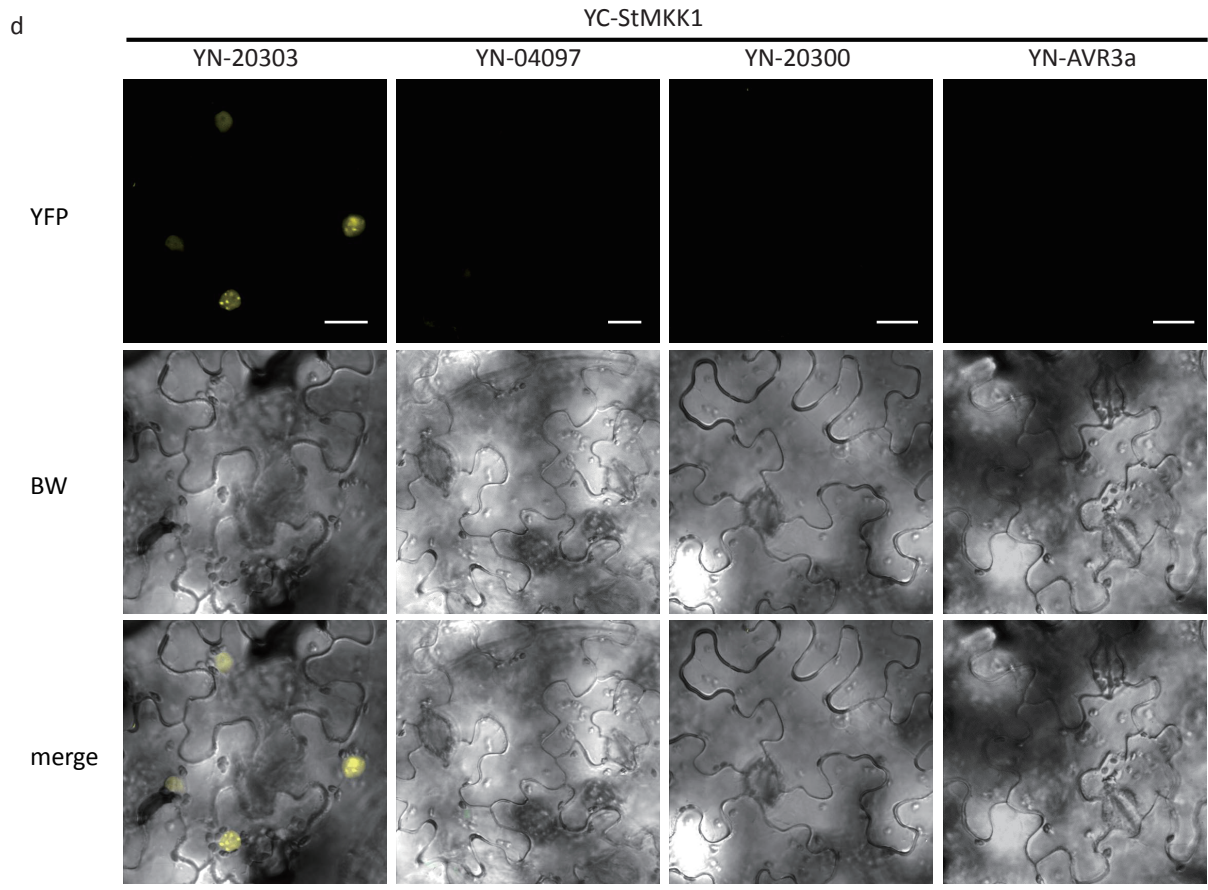
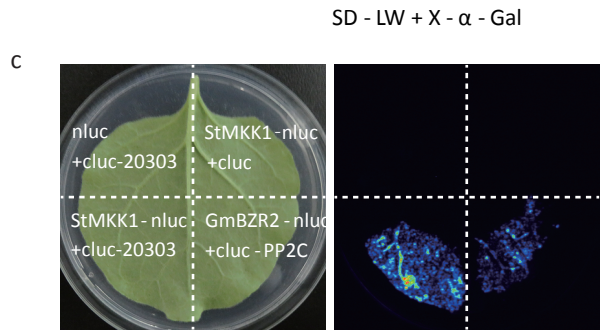
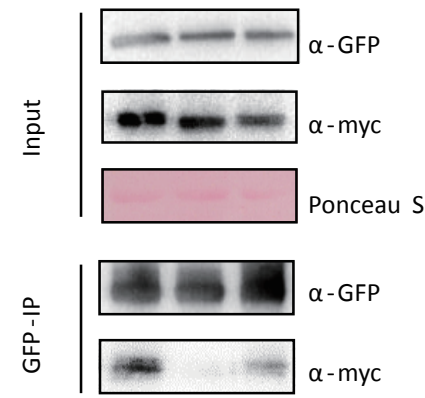
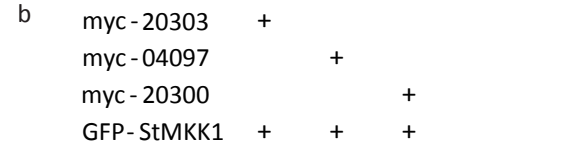
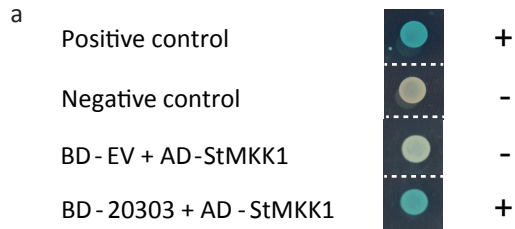
Figure 6. *GFP-20303NLS* depends on *NbMKK1* in promoting *P. infestans* colonization. *GFP* and *GFP-20303NLS* (a, b) or *GFP* and *GFP-20303* (c, d) were agroinfiltrated into the left and right panels of *TRV-GUS* and *TRV-MKK1* leaves. Zoospores of *P. infestans* isolate 14-3-GFP were inoculated onto the agroinfiltrated leaves at 1 day post infiltration (dpi), and lesion diameters were measured at 5 dai. a and c, The bar graphs showing the mean lesion areas in mm². Error bars show SE from 12 replicates. Asterisks indicate significant differences ($n \geq 12$; one-sided

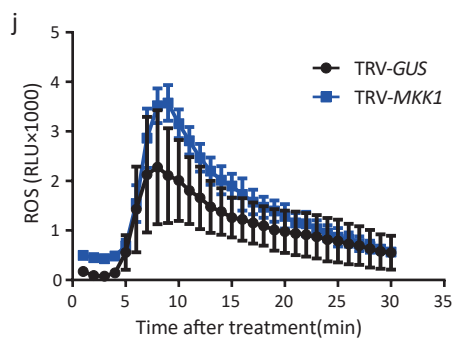
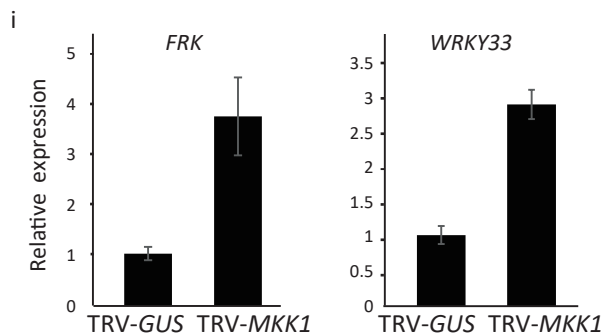
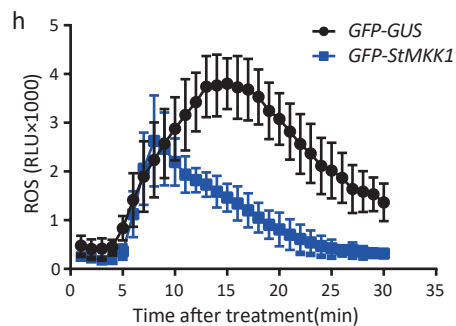
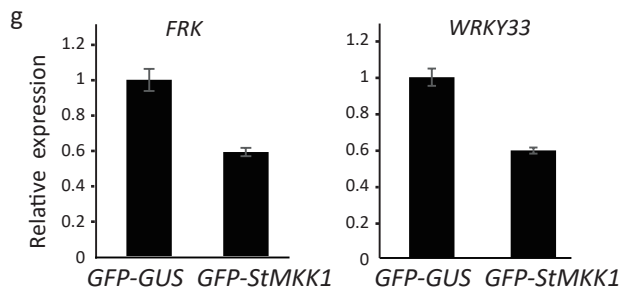
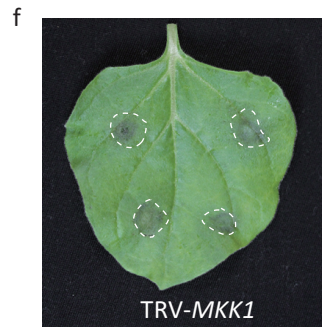
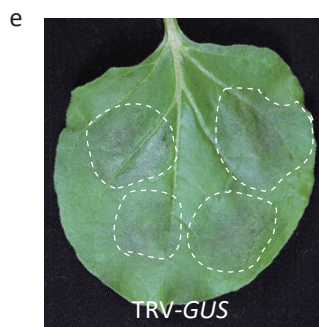
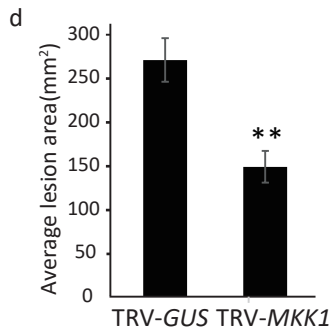
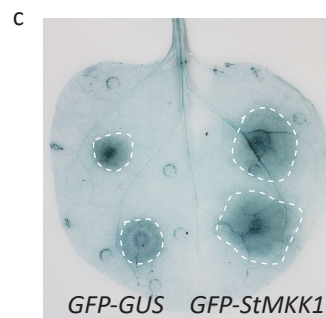
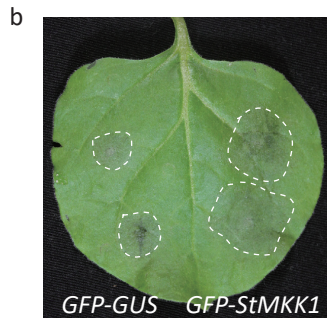
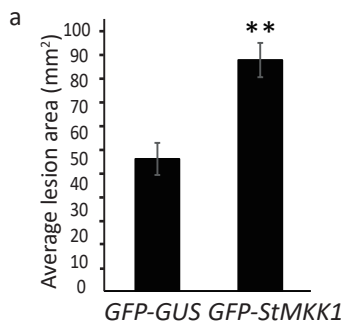
Student's t-test, $P \leq 0.01$). b and d, Blue light pictures showing lesion developments at 5 dai. Lesion areas were indicated with dotted circle. The experiments were repeated two times with similar results.

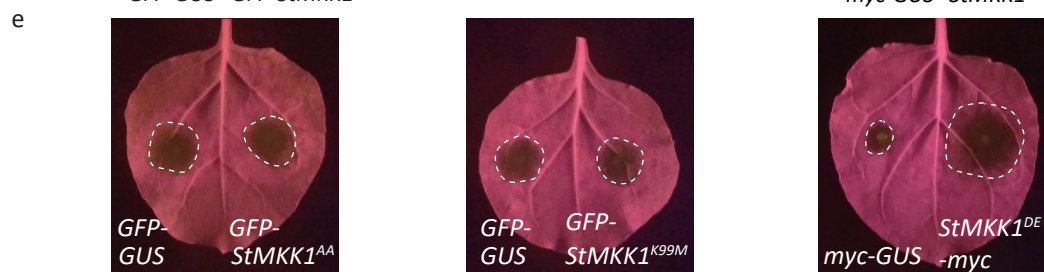
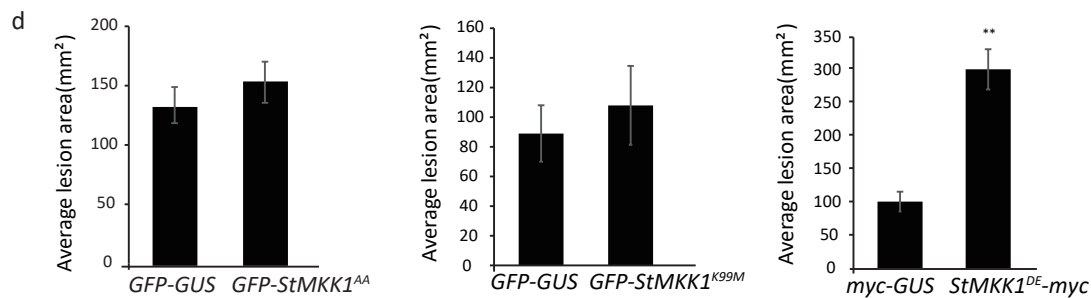
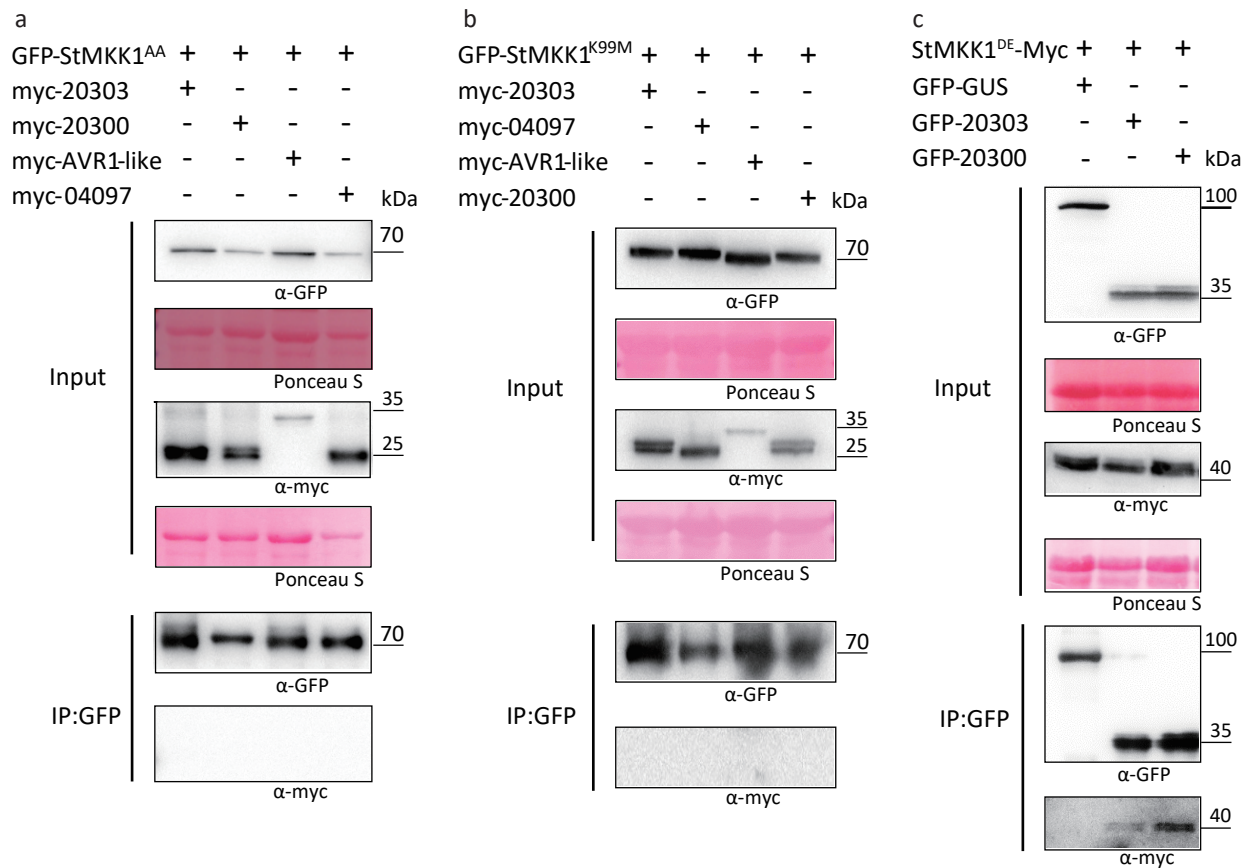
Figure 7. StMKK1 is stabilized by PITG20303 and PITG20300. a, Proteins were extracted at 2 dpi from *N. benthamiana* leaves co-expressing *GFP-StMKK1* and *myc-20303* or *GFP-StMKK1* and *myc-GUS* with and without 10 μ M flg22 treatment at 1 dpi. b, Proteins were extracted at 2 dpi from leaves co-expressing *myc-StMKK1* with *GFP-20303*, *GFP-20300* or *GFP* treated with MG132 or its solvent DMSO at 12 hpi. GFP- and myc- fusion proteins were detected by western blots with GFP- and myc- antibodies respectively. The experiments were repeated three times with similar results. +, indicated the expression of proteins in the leaves. Protein loading is indicated by Ponceau stain (Ponceau S). Numbers indicate the relative intensity of StMKK1 bands normalized to Rubisco.

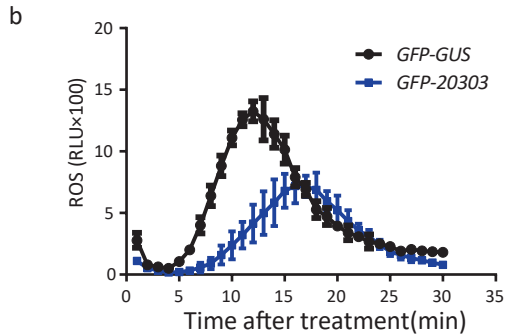
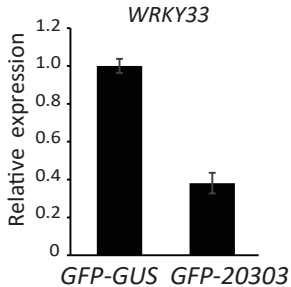
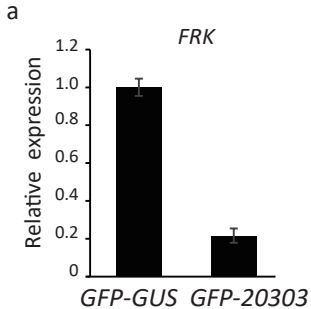
Figure 8. *P. infestans* RXLR effector PITG20303 targets and stabilizes the potato StMKK1 protein. The model shows upon *P. infestans* colonization, effectors PITG20300 and PITG20303 are secreted and translocated into the host cell, where PITG20300 inhibits the secretion of C14 at the plasma membrane. In the host nucleus these two effectors target and stabilize the potato StMKK1 protein to interfere with plant PTI. StMKK1 suppresses plant PTI responses as indicated by the suppression of *FRK* and *WRKY33* expression and ROS burst.

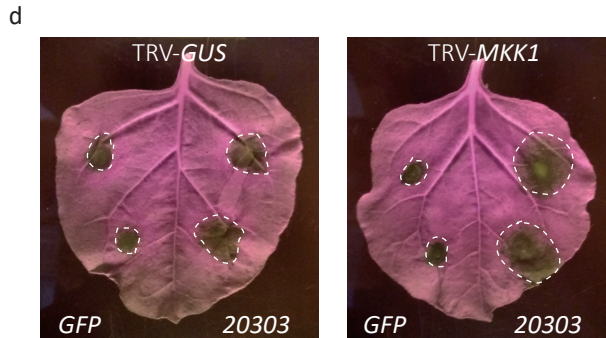
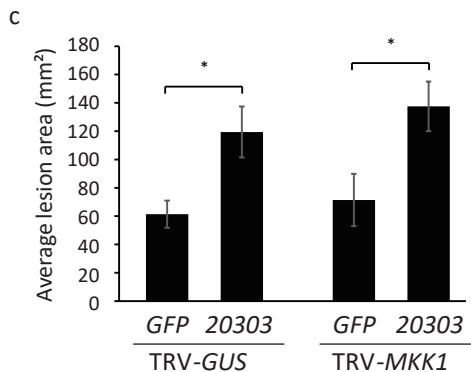
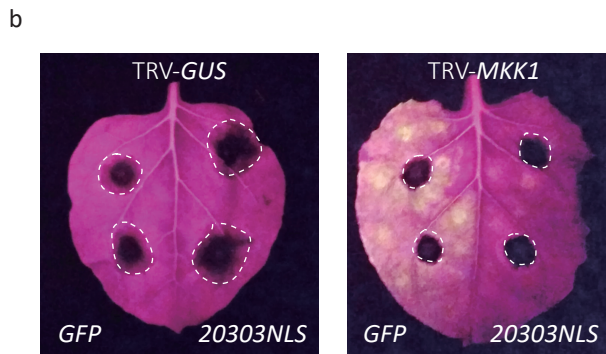
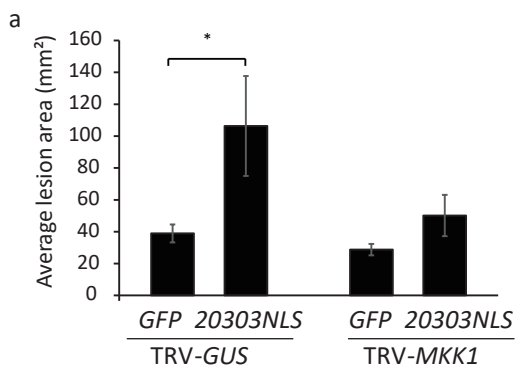
a**b****c**





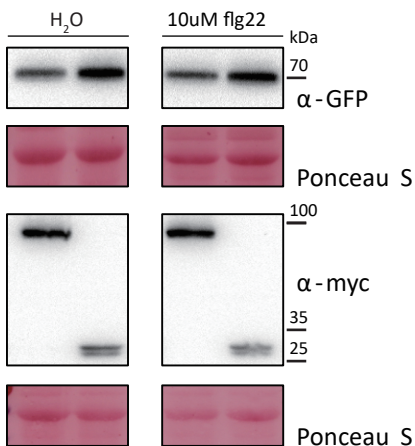






a

GFP-StMKK1	+	+	+	+
myc-GUS	+	-	+	-
myc-20303	-	+	-	+



b

